







Independent Real and Imaginary Spectral Analysis for Improving the Brillouin Frequency Shift Resolution in the Differential Cross-Spectrum BOTDR (DCS-BOTDR) Fiber Sensor

Ain Nabihah Mohammad Rihan¹^a, Mohd Saiful Dzulkefly Zan¹^b, Yosuke Tanaka²^c,
Mohd Hadri Hafiz Mokhtar¹^d, Norhana Arsad¹^e and Ahmad Ashrif A Bakar¹^f
¹Department of Electrical, Electronic & Systems Engineering, Faculty of Engineering & Built Environment,
Universiti Kebangsaan Malaysia, 43600 UKM Bangi, Selangor Darul Ehsan, Malaysia
²Department of Electrical and Electronic Engineering, Graduate School of Engineering,
Tokyo University of Agriculture and Technology, Koganei, Tokyo 184-8588, Japan


Keywords: Distributed Fiber Sensor, Strain and Temperature Sensor, Brillouin Optical Time Domain Reflectometry, Spectral Analysis, Fast Fourier Transform.


Abstract: We propose a technique to improve Brillouin gain spectrum (BGS) acquisition in a Brillouin optical time domain reflectometry (BOTDR) fiber sensor by independently analyzing the real and imaginary components of the Brillouin backscattered signal through fast Fourier transform (FFT) analysis. This technique aims to enhance Brillouin frequency shift (BFS) resolution in our previously proposed differential cross-spectrum BOTDR (DCS-BOTDR) method. Using an intensity modulation scheme to generate a probe pulse pair, we conducted temperature sensing experiment by heating an 8 m section at the far end of a 1.2 km fiber at 70°C. The experimental results showed a significant reduction of BGS width from 128 MHz to around 53 MHz with the real spectrum component. Consequently, this has resulted in the enhancement of the BFS resolution to 1.49 MHz using the real spectrum and 1.51 MHz with the imaginary spectrum. We have also achieved 40 cm spatial resolution measurement and reduced the processing time from 7.21 s to 7.08 s, demonstrating an improved efficiency and accuracy for distributed temperature measurement in BOTDR sensor.


1 INTRODUCTION


In recent years, many studies on Brillouin optical time domain reflectometry (BOTDR) have multiplied due to its potential applications such as structural health monitoring of large infrastructures, pipeline monitoring, and power cable monitoring. The growing interest was influenced by the ability of BOTDR systems to detect local variations in Brillouin frequency shift that are sensitive to temperature and strain, which allows for distributed


sensing. As a result of the linear dependence of temperature and strain on the Brillouin frequency shift (BFS), the Brillouin gain spectrum mapping was used for distributed temperature and strain sensing in the BOTDR system (Bao et al., 2021). The BOTDR system utilized spontaneous Brillouin scattering (SpBS) to measure the strain distribution. However, signal-to-noise (SNR) is weak due to the low amplitude of the SpBS. The SNR can be improved by increasing the pulse width, but the spatial resolution will be compromised.


^a <https://orcid.org/0009-0004-8101-1197>

^b <https://orcid.org/0000-0002-1440-5434>

^c <https://orcid.org/0000-0002-6539-5977>

^d <https://orcid.org/0000-0001-5307-073X>

^e <https://orcid.org/0000-0003-4543-8383>

^f <https://orcid.org/0000-0002-9060-0346>

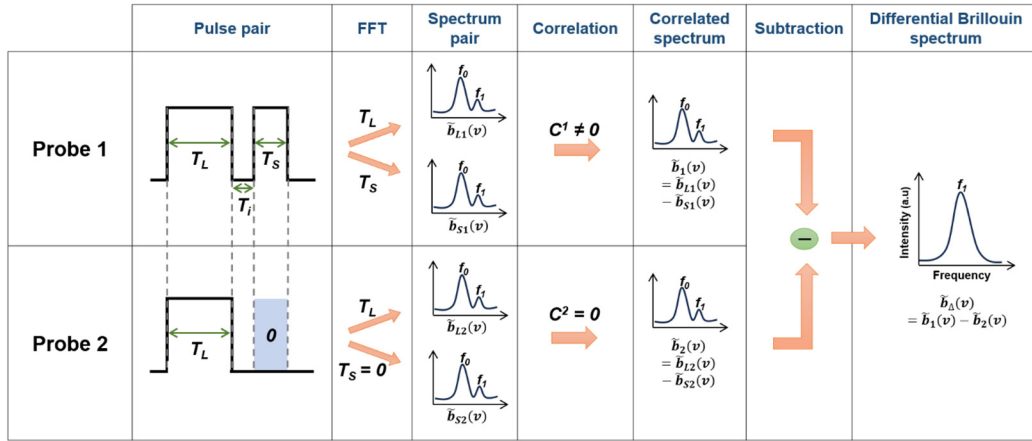


Figure 1: Time domain Brillouin backscattered (BS) analysis scheme using differential cross spectrum technique.

Due to the trade-off between these parameters, various studies have been conducted on enhancing spatial resolution without compromising the SNR (Almoosa et al., 2022; Horiguchi et al., 2019; Zan et al., 2018). Almoosa et. al proposed a method to improve the BFS resolution of the BOTDR system by using an artificial neural network (ANN) (Almoosa et al., 2022). This technique demonstrated the improvement of BFS resolution from 21.13 MHz to 2.88 MHz. Horiguchi et. al reported phase shift pulse BOTDR (PSP-BOTDR) where a probe pulse pair modulated by the phase shift keying method and has obtained 20 cm spatial resolution with this method (Horiguchi et al., 2019). Differential cross-spectrum BOTDR (DCS-BOTDR) which has a similar approach to the PSP-BOTDR was proposed by Zan et al. (2018), whereby an intensity modulation scheme is used to generate a long-short probe pulse pair. This technique has demonstrated 0.2 m spatial resolution for a 350 m sensing range. Even though all of these techniques have further improved the spatial resolution of the BOTDR system, the measurement time took quite a long period due to high averaging.

In this paper, we introduce a method to acquire the BGS by independently analysing real and imaginary parts of the fast Fourier transform (FFT). In the DCS-BOTDR, the BGS was acquired by analysing power spectral density (PSD), which is the magnitude of real and imaginary components. The proposed method will use a similar intensity modulation scheme of the DCS-BOTDR to modulate the long-short probe pulse pair, but use a different approach to extract the BGS. This experiment will focus on independent analysis to effectively improve the BFS resolution while also successfully reducing the measurement time.

2 PRINCIPLES

2.1 Real and Imaginary Spectrum of DCS-BOTDR

In a conventional BOTDR system, the Brillouin spectrum was extracted from the backscattered signal in the frequency domain by applying the FFT. Fundamentally, the FFT is an algorithm that calculates fast discrete Fourier transform (DFT) (Smith, 1997). The DFT converts the time domain signal into a frequency domain that yields two components; real and imaginary. Hence, the DCS-BOTDR method introduces a cross-correlation method by calculating the complex conjugate of both components of the FFT to acquire the PSD. Considering that both real and imaginary parts of the FFT can work independently, the spectrum analysis to compare three different spectra; conventional, real, and imaginary was conducted based on the DCS-BOTDR method.

Figure 1 provides an overview of the key steps involved in this method, starting from the generation of probe pulses to the computation of the differential Brillouin spectrum. As illustrated, two probe pulses are utilized which both probes have a long pulse duration (T_L), but only Probe 1 includes a short pulse duration (T_S), separated by an interval duration (T_i) between and Probe 2 serves as a reference. Initially, the backscattered signal in the time domain can be expressed as $\tilde{b}(t_0, z)$, where z is the position in the optical fiber and t_0 refers to the reference time. After converting to the frequency domain by performing the FFT, the backscattered signal will yield both real and imaginary components, expressed as:

$$\tilde{B}(f, z) = Re\{\tilde{B}(f, z)\} + Im\{\tilde{B}(f, z)\} \quad (1)$$

where $\tilde{B}(f, z)$ represents the backscattered signal in the frequency domain at the position z , Re refers to the real part that corresponds to cosine components, while Im refers to the imaginary part that corresponds to the sine components. Then, cross-correlation as depicted in Figure 1 involves calculating the interaction between the backscattered signals between Probe 1 ($\tilde{b}_L(t_0, z)$) and Probe 2 ($\tilde{b}_S(t_0, z)$) in the frequency domain. This is computed and described as follows:

$$Re\{C_{rr}(\tau, t_0, z)\} = \sum \left[\begin{array}{l} Re\{\tilde{b}_L(f, z)\}Re\{\tilde{b}_S(f, z)\} \\ +Im\{\tilde{b}_L(f, z)\}Im\{\tilde{b}_S(f, z)\} \end{array} \right] \quad (2)$$

$$Im\{C_{rr}(\tau, t_0, z)\} = \sum \left[\begin{array}{l} Im\{\tilde{b}_L(f, z)\}Re\{\tilde{b}_S(f, z)\} \\ -Re\{\tilde{b}_L(f, z)\}Im\{\tilde{b}_S(f, z)\} \end{array} \right] \quad (3)$$

Equation 2 and 3 represent the correlation between real and imaginary components of the backscattered signals from both probes. They also signify the interaction of the two signals in the frequency domain. These equations also yield the real and imaginary part of the Brillouin spectrum. “Subtraction” and “Differential Brillouin Spectrum” columns in Figure 1 depict the subsequent step computes the magnitude of the cross-spectrum to determine the PSD of the cross-correlated signal in the frequency domain. The magnitude of cross-spectrum is also defined as the conventional spectrum deployed in the DCS-BOTDR technique and it can be calculated as:

$$\begin{aligned} & |\tilde{C}_{rr}(\tau, t_0, z)| \\ &= \sqrt{Re\{\tilde{C}_{rr}(\tau, t_0, z)\}^2 + Im\{\tilde{C}_{rr}(\tau, t_0, z)\}^2} \end{aligned} \quad (4)$$

This magnitude combines both real and imaginary parts and gives the measure of the PSD in the frequency domain. The steps outlined in Figure 1 ensure that both components are utilized effectively, leading to an improved understanding and accuracy of the Brillouin spectrum.

2.2 Zero-Crossing Point Search

To find the BFS for the imaginary spectrum, a zero-crossing point search (ZCPS) is applied instead of a maximum peak search. This is because the frequency of the zero-crossing point for the imaginary spectrum is equivalent to the frequency for the real and conventional spectra (see Figure 2). The ZCPS is adapted from Nonogaki et al. (2024) which has proposed this method for a Brillouin optical time

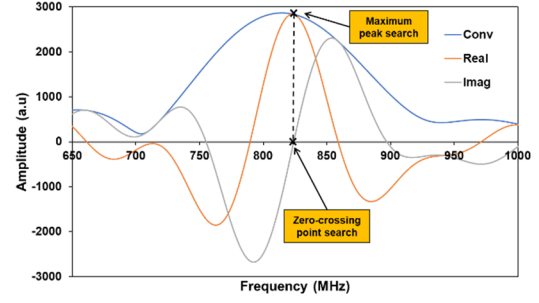


Figure 2: BGS of real, imaginary, and conventional spectrum.

domain analyzer (BOTDA) system. The BGS of the imaginary part can be explained as:

$$f_{zero} = -\frac{b_{BGS}}{a_{BGS}} \quad (5)$$

where a_{BGS} refers to the slope of the linear regression between the maximum and minimum values of the BGS, and b_{BGS} is the intercept of the linear regression. The slope of the linear regression which can be denoted as a gradient m can also determine the linearity between the BGS of heated and unheated BGS which will be discussed in the next section.

3 EXPERIMENTAL ANALYSIS

3.1 Experimental Setup

The configuration of the experimental setup is depicted in Figure 3. Continuous light of 1550 nm wavelength with 12 dBm input power was upshifted and downshifted by frequency modulation scheme. A synthesized signal generator (SSG) supplied a 10 GHz sinusoidal wave to a Mach-Zehnder modulator (MZM) for frequency shift keying. Arbitrary waveform generator (AWG) modulates the incoming optical signal to generate the optical pulses as shown in Figure 1. By using acousto-optic modulation (AOM), optical pulses were generated via ON-OFF keying modulation. Then, the AWG was set to produce the desired electric pulses such that $T_L = 10$ ns, $T_S = 4$ ns, and $T_i = 2$ ns. Two optical amplifiers (EDFA 1 and EDFA 2) were incorporated into the setup to compensate insertion loss, with input currents of 180 mA and 80 mA respectively. The overall output power detected by oscilloscope (OSC) was measured to be 600 mW. The experiment was carried out using a total fiber length of 1.2 km, with a heated section placed inside a water bath approximately 8 meters near the far end of the fiber, at a fixed temperature of 70°C. The SpBS that

consists of both Brillouin gain and loss spectra in the optical fiber were generated by the optical pulses for temperature measurement.

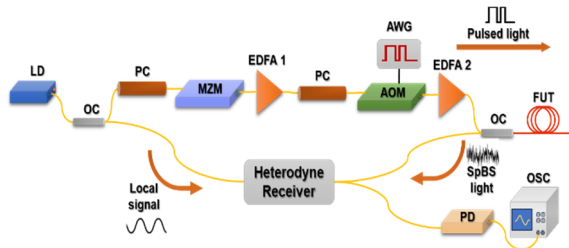


Figure 3: Schematic experimental setup of DCS-BOTDR. LD: laser diode, OC: optical coupler, PC; polarization controller, MZM: Mach-Zehnder modulator, EDFA: erbium-doped fiber amplifier, AOM: acousto-optic modulator, AWG: arbitrary waveform generator, PD: photodetector, OSC: oscilloscope, FUT: fiber-under-test, SpBS: spontaneous Brillouin scattering.

3.2 Results and Analysis

Figure 4 shows three different Brillouin spectra; real, imaginary, and conventional, acquired using the proposed technique. The measurement was monitored at $z = 1.2$ km for both heated and unheated fiber sections along the FUT. All Brillouin spectra recorded the same frequency shift at around 46 MHz. In comparison with the frequency shift, the spectral bandwidth of the BGS calculated at full-width-half-maximum (FWHM) shows an improvement compared to the conventional one. As can be seen in Figure 4 (a), the conventional spectrum of the heated section has a broad spectrum width of 128 MHz. In contrast, a narrower bandwidth of 53 MHz as depicted in Figure 4 (b), was achieved when only the real part of the FFT analysis was considered during the spectral analysis of the time domain signal.

In most cases, the Brillouin spectrum typically exhibits a Lorentzian line shape with a symmetrical peak due to lifetime broadening, which makes it possible to measure the FWHM (Antonacci et al., 2013). Meanwhile, the imaginary spectrum usually does not conform to a Lorentzian shape as evident in Figure 4 (c) because it may exhibit multiple peaks, unlike the real and conventional spectra. Consequently, relying on the FWHM analysis for the imaginary spectrum may increase inaccuracies in the calculation that potentially affect the reliability of the result. Another method to evaluate the imaginary spectrum involves comparing the linearity of Brillouin spectrum slopes between the heated and unheated spectra.

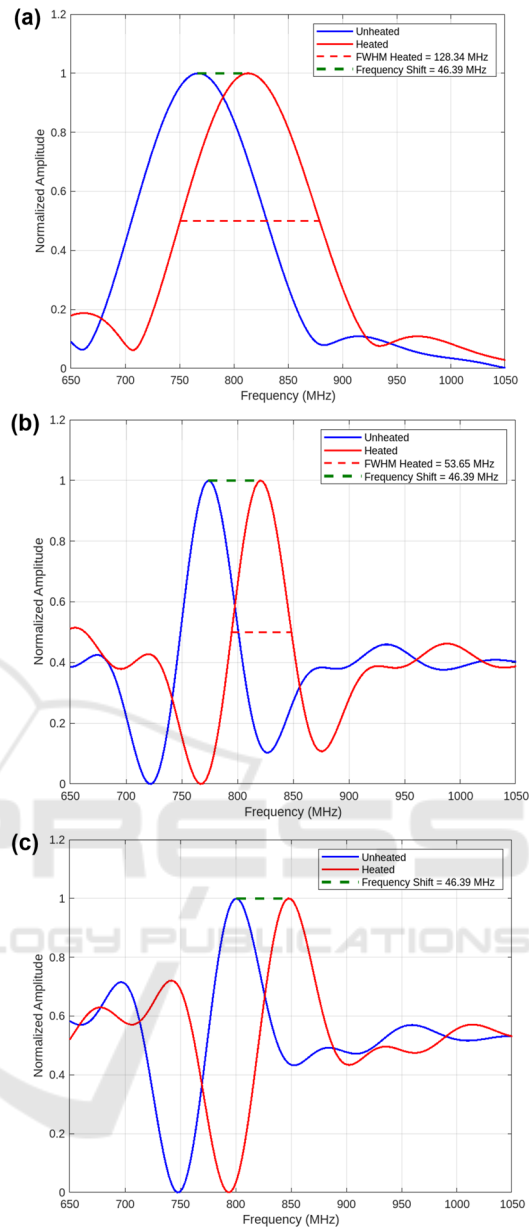


Figure 4: Brillouin spectrum at the heated and unheated section of 1 km for (a) conventional, (b) real, and (c) imaginary spectrum.

Previously, Peng et al. (2022) conducted a similar method known as double-slope assisted BOTDR (DSA-BOTDR) to study the linear dependence of the Brillouin spectrum on temperature and evaluate the sensitivity of the BOTDR system to temperature variations. Based on Figure 4 (c), the unheated and heated spectra have small differences in slopes, with values of 0.008 and 0.009 respectively. This difference suggests an increased sensitivity to temperature changes and the

Brillouin spectrum shifted more rapidly under heated conditions. The small difference in slopes suggests that the system maintains stability and consistency across different thermal conditions. Figures 5 (a) and (b) show the BFS distribution monitored at the 70°C heated section of the FUT. From Figure 5 (a), it was found that the spatial resolution analyzed at the 8 m fiber section was 40 cm and the BFS was approximately 50 MHz. By calculating the standard deviation, the BFS resolution can be determined more accurately, thanks to the narrowed Brillouin spectrum of the real components and the linear slope from the imaginary component. The measured BFS resolutions for real, imaginary, and conventional spectra were 1.49 MHz, 1.51 MHz, and 3.24 MHz, respectively. This confirms that the BFS resolution can be improved by employing independent real or imaginary components for FFT analysis to extract the Brillouin spectrum. Finally, the time taken to extract the Brillouin spectrum from the backscattered signal through FFT analysis was analyzed.

In our experiment, we averaged the data 20,000 times and conducted FFT analysis on a total of 576 BGS spectra, monitored from 1 km to the fiber end for each type of spectrum (real, imaginary, and conventional). The processing time required to compute one BGS for the real, imaginary, and conventional categories are 7.09s, 7.08s, and 7.21s, respectively. Concentrating on the independent computation of either the real or imaginary components of the BGS for FFT analysis can significantly reduce processing time. In comparison with previous works, Table 1 shows the improvement of the experimental results based on the spatial resolution and BFS resolution.

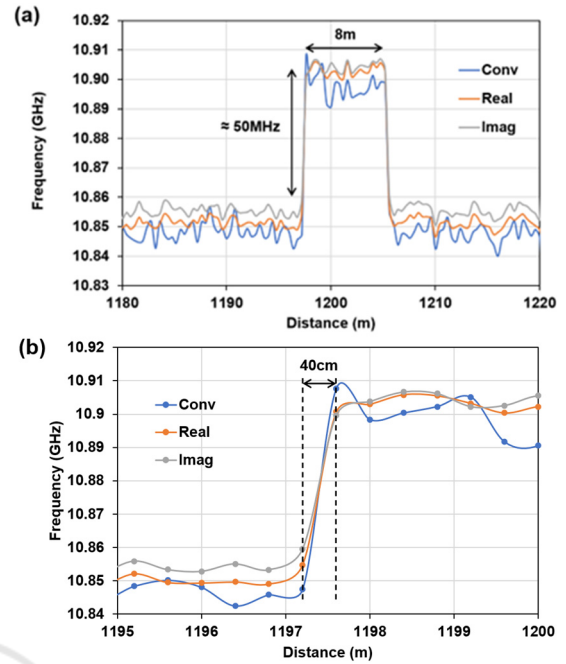


Figure 5: BFS distribution comparison of real, imaginary, and conventional spectrum. (a) Temperature distribution at 8 m heated section. (b) Spatial resolution of the BFS distribution.

4 CONCLUSIONS

In this paper, we propose a technique to acquire the Brillouin gain spectrum (BGS) by independently analyzing the real and imaginary components of the Brillouin backscattered signal. The experiment was conducted using DCS-BOTDR intensity modulation scheme to generate a probe pulse pair. The

Table 1: Performance specifications of different DCS-BOTDR schemes.

Ref.	Method	Results	
		Spatial resolution (m)	BFS (MHz)
Zan et al. (2018)	Differential cross spectrum (DCS)	0.2	3.20
Zan et al. (2020)	Golay coded pulse coding	0.4	3.47
Almoosa et al. (2022)	Artificial neural network (ANN)	0.4	2.88
Zan et al. (2022)	Effect of pulse duration	0.4	$\pm 1-2$ MHz (longer pulse durations) ± 0.5 MHz (shorter pulse durations)
This work	Independent real and imaginary spectral analysis	0.4	1.49 (real) 1.52 (imaginary)

experiment results show that separating these components enhanced the Brillouin frequency shift (BFS) resolution, with the conventional spectrum width improved from 128 MHz to 53 MHz using the real spectrum. Additionally, temperature sensitivity was demonstrated by comparing heated and unheated imaginary spectra. A 50 MHz BFS shift, 40 cm spatial resolution, and reduced processing time from 7.21s to 7.08s were achieved.

Zan, M. S. D., Mokhtar, M. H. H., Elgaud, M. M., Bakar, A. a. A., Arsad, N., & Mahdi, M. A. (2020). *Pulse Coding Technique in Differential Cross-Spectrum BOTDR for Improving the Brillouin Frequency Accuracy and Spatial Resolution* (pp. 11–12).

ACKNOWLEDGEMENTS

This research was supported by the Fundamental Research Grant Scheme (FRGS) from the Ministry of Higher Education of Malaysia (MOHE): Grant No. FRGS/1/2023/TK07/UKM/02/2.

REFERENCES

- Almoosa, A. S. K., Hamzah, A. E., Zan, M. S. D., Ibrahim, M. F., Arsad, N., & Elgaud, M. M. (2022). Improving the Brillouin frequency shift measurement resolution in the Brillouin optical time domain reflectometry (BOTDR) fiber sensor by artificial neural network (ANN). *Optical Fiber Technology*, 70, 102860.
- Antonacci, G., Foreman, M. R., Paterson, C., & Török, P. (2013). Spectral broadening in Brillouin imaging. *Applied Physics Letters*, 103(22).
- Bao, X., Zhou, Z., & Wang, Y. (2021). Review: distributed time-domain sensors based on Brillouin scattering and FWM enhanced SBS for temperature, strain and acoustic wave detection. *Photonix*, 2(1).
- Horiguchi, T., Masui, Y., & Zan, M. S. D. (2019). Analysis of Phase-Shift Pulse Brillouin Optical Time-Domain reflectometry. *Sensors*, 19(7), 1497.
- Nonogaki, H., Sei, D., Zan, M. S. D., & Tanaka, Y. (2024). Brillouin frequency shift measurement by zero-crossing point search in virtually synthesized spectra of Brillouin gain and loss. *Applied Physics Express*.
- Peng, J., Lu, Y., Zhang, Y., Wu, Z., & Zhang, Z. (2022). Double-Slope assisted Brillouin optical time domain reflectometry with linear regions merging. *IEEE Photonics Technology Letters*, 34(15), 819–822.
- Smith, S. W. (1997). *The scientist and engineer's guide to digital signal processing*. California Technical Pub.
- Zan, M. S. D., Almoosa, A. S. K., Ibrahim, M. F., Elgaud, M. M., Hamzah, A. E., Arsad, N., Mokhtar, M. H. H., & Bakar, A. a. A. (2022). The effect of pulse duration on the Brillouin frequency shift accuracy in the differential cross-spectrum BOTDR (DCS-BOTDR) fiber sensor. *Optical Fiber Technology*, 72, 102977.
- Zan, M. S. D., Masui, Y., & Horiguchi, T. (2018). Differential Cross Spectrum Technique for Improving the Spatial Resolution of BOTDR Sensor. In *2018 IEEE 7th International Conference on Photonics (ICP)*.